XLI CILAMCE
XLI Ibero-Latin American Congress on Computational Methods in Engineering
16-19 November, 2020 FOZ DO IGUAÇU PARANÁ – BRAZIL

Numerical modeling of cable-rigid-body structural systems using the NP-FEM method

Mateus Guimarães Tonin [1], Alexandre Luis Braun [1]

[1] *Programa de Pós-Graduação em Engenharia Civil, Universidade Federal do Rio Grande do Sul*
Av. Osvaldo Aranha 99, 90035-190, Porto Alegre - RS, Brazil
mateus.tonin@ufrgs.br, alexandre.braun@ufrgs.br

Abstract. This work presents a numerical formulation based on the Finite Element Method (FEM) to solve non-linear dynamic problems involving cable-rigid-body structural systems. The Nodal Position Finite Element Method (NP-FEM), used for cable modeling, is a simple and robust method that resolves directly the position of cable nodes instead of indirectly using displacements. In this way, a polar decomposition of the cable elastic deformations and rigid body rotations are not necessary, eliminating errors in the incremental approximations existing in classic FEM formulations. The method is suitable for simulating cables with large rigid body rotations and small elastic axial deformations. The body linked to the cable is treated as a rigid body with six degrees of freedom and the cable-rigid-body coupling is done by creating an extra, massless, cable element with a very large axial rigidity to simulate the rigid link between the cable free end and the center of gravity (CG) of the rigid body. The algorithm is verified through comparisons with other authors, using their own numerical codes or commercials software, and experimental predictions. Results are very close to those of the references and proved that the formulation proposed here is quite efficient, reliable and stable for the examples simulated.

Keywords: Cable-rigid-body interaction; Nonlinear dynamics; NP-FEM.

1 Introduction

Cable-like structures appear in a large number of applications in science, industry and defense, as showed by Sun et al. [1]. This is mainly because of their versatility: they are capable of transmitting forces, carrying payloads and conducting electrical power and signals (See Ding et al. [2]).
As showed by Zhu [3], the dynamics of towed cable systems can be formulated by four different methods: analytical, lumped parameter, Finite Difference Method (FDM) and Finite Element Method (FEM).
The main advantage of FEM is that it can be implemented in a general-purpose analysis program to handle complex cable systems (Zhu [3]), like in multiple cable branches or cables with variable properties along its length (Ding et al. [2]). Unfortunately, the FEM method wasn't widely adopted in cable dynamics, mainly because: (1) the FEM calculates relative displacements instead of positions; and (2) the method also requires a decoupling between the large rigid body displacements and rotations and the small elastic stretch, which creates accumulated numerical errors over time (Sun et al. [1]).
The Nodal Position Finite Element Method (NP-FEM), developed by Zhu [3], replaces the nodal displacements in the conventional FEM by nodal positions (Ding et al. [4]). The recently new method is capable of eliminating the decoupling of the rigid body rotation and the elastic deformation of the element in large rigid body rotations; and, consequently the accumulating numerical errors resulting from the solution at each time step (Sun et al. [1]). The relatively new NP-FEM has been implemented into a simulation program together with the rigid body dynamics of the towed body.

2 Formulation of NP-FEM

Initially, consider the two-noded straight cable element in a three-dimensional space, showed in Fig. 1. The element geometry is described by its nodal coordinates (X_i, Y_i, Z_i) (i=1, 2) in a global coordinate system $OXYZ$ and (x_i, y_i, z_i) (i=1, 2) in local coordinates x, y and z, where the x-axis is defined along the cable, y- and z-axes are perpendicular to the x-axis, respectively (Sun et al. [1]).

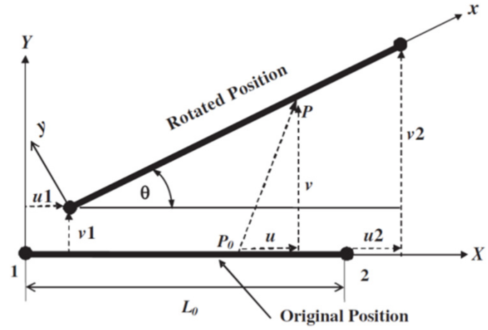

Figure 1. Cable element in large rigid body rotation (Zhu [3])

The position, velocity and acceleration of an arbitrary point along the cable element can be expressed in terms of element shape functions and the corresponding nodal values, in the form:

$$\boldsymbol{R} = \boldsymbol{N}\boldsymbol{X}_{\boldsymbol{e}},\ \ \boldsymbol{v} = \dot{\boldsymbol{R}} = \boldsymbol{N}\dot{\boldsymbol{X}}_{\boldsymbol{e}},\ \ \boldsymbol{a} = \ddot{\boldsymbol{R}} = \boldsymbol{N}\ddot{\boldsymbol{X}}_{\boldsymbol{e}},\ \boldsymbol{N} = \begin{bmatrix} 1-\zeta & 0 & 0 & \zeta & 0 & 0 \\ 0 & 1-\zeta & 0 & 0 & \zeta & 0 \\ 0 & 0 & 1-\zeta & 0 & 0 & \zeta \end{bmatrix}, \tag{1}$$

$$\zeta = \frac{\sqrt{\left(X - X_1\right)^2 + \left(Y - Y_1\right)^2 + \left(Z - Z_1\right)^2}}{\sqrt{\left(X_2 - X_1\right)^2 + \left(Y_2 - Y_1\right)^2 + \left(Z_2 - Z_1\right)^2}}, \tag{2}$$

where $\boldsymbol{R} = \left\{X,\ Y, Z\right\}^T$, $\boldsymbol{v} = \left\{v_x,\ v_y,\ v_z\right\}^T$ and $\boldsymbol{a} = \left\{a_x,\ a_y,\ a_z\right\}^T$ are the position, velocity and acceleration vectors of the arbitrary point in the global coordinate system, respectively, $\boldsymbol{X}_{\boldsymbol{e}} = \left\{X_1, Y_1, Z_1, X_2, Y_2, Z_2\right\}^T$ is the global nodal coordinates at the current time, $\boldsymbol{N}$ is the element shape function matrix and the dot denotes the time derivatives, respectively (Sun et al. [1]).

In a total Lagrangian description, the deformation of the cable element is defined by:

$$u = x - x_0, \tag{3}$$

where x_0 and x are the coordinates of an arbitrary point along the element before and after deformation, respectively.

The Green-Lagrange strain component ε_x at element level is defined as (Zhu [3]):

$$\boldsymbol{\varepsilon}_x = \frac{L}{L_0} - 1 = \frac{X_2 - X_1}{L_0}\cos\boldsymbol{\theta}_x + \frac{Y_2 - Y_1}{L_0}\cos\boldsymbol{\theta}_y + \frac{Z_2 - Z_1}{L_0}\cos\boldsymbol{\theta}_z - 1 = \boldsymbol{B}\boldsymbol{X}_{\boldsymbol{e}} - 1, \tag{4}$$

where L and L_0 are the length of the deformed and undeformed element and the directional cosines are defined as (Zhu [3]):

$$\cos\boldsymbol{\theta}_x = \frac{X_2 - X_1}{L},\ \ \cos\boldsymbol{\theta}_y = \frac{Y_2 - Y_1}{L},\ \ \cos\boldsymbol{\theta}_z = \frac{Z_2 - Z_1}{L}. \tag{5}$$

The strain matrix $\boldsymbol{B}$ is defined as (Zhu [3]):

$$\boldsymbol{B} = \left[-\frac{\cos\boldsymbol{\theta}_x}{L_0}, -\frac{\cos\boldsymbol{\theta}_y}{L_0}, -\frac{\cos\boldsymbol{\theta}_z}{L_0}, \frac{\cos\boldsymbol{\theta}_x}{L_0}, \frac{\cos\boldsymbol{\theta}_y}{L_0}, \frac{\cos\boldsymbol{\theta}_z}{L_0}\right], \tag{6}$$

which can be further decomposed into the product of the strain matrix in the local coordinates $\boldsymbol{B_0}$ and the coordinate transformation matrix $\boldsymbol{Q}$, such as (Zhu [3]):

$$\boldsymbol{B} = \boldsymbol{B_0}\boldsymbol{Q}, \tag{7}$$

where:

$$\boldsymbol{B_0} = \left[-\frac{1}{L_0},\ 0,\ 0,\ \frac{1}{L_0},\ 0,\ 0 \right], \boldsymbol{Q} = \begin{bmatrix} \cos\theta_x & \cos\theta_y & \cos\theta_z & 0 & 0 & 0 \\ 0 & 0 & 0 & 0 & 0 & 0 \\ 0 & 0 & 0 & 0 & 0 & 0 \\ 0 & 0 & 0 & \cos\theta_x & \cos\theta_y & \cos\theta_z \\ 0 & 0 & 0 & 0 & 0 & 0 \\ 0 & 0 & 0 & 0 & 0 & 0 \end{bmatrix}. \tag{8}$$

Once the element kinematics has been established, the element mass and stiffness matrices, as well as the nodal force vectors are defined as (Zhu [3]):

$$\boldsymbol{M} = \frac{\rho AL}{6} \begin{bmatrix} 2 & 0 & 0 & 1 & 0 & 0 \\ 0 & 2 & 0 & 0 & 1 & 0 \\ 0 & 0 & 2 & 0 & 0 & 1 \\ 1 & 0 & 0 & 2 & 0 & 0 \\ 0 & 1 & 0 & 0 & 2 & 0 \\ 0 & 0 & 1 & 0 & 0 & 2 \end{bmatrix}, \tag{9}$$

$$\boldsymbol{K} = EAL\left(\boldsymbol{B_0 Q}\right)^T \boldsymbol{B_0 Q} = \boldsymbol{Q}^T \boldsymbol{K_0 Q},\ K_0 = \frac{EAL}{L_0^2} \begin{bmatrix} 1 & 0 & 0 & -1 & 0 & 0 \\ 0 & 0 & 0 & 0 & 0 & 0 \\ 0 & 0 & 0 & 0 & 0 & 0 \\ -1 & 0 & 0 & 1 & 0 & 0 \\ 0 & 0 & 0 & 0 & 0 & 0 \\ 0 & 0 & 0 & 0 & 0 & 0 \end{bmatrix}, \tag{10}$$

$$\boldsymbol{C} = \beta\boldsymbol{M} + \gamma\boldsymbol{K}, \boldsymbol{F}_g = -\frac{LA\rho g}{2}\left\{0,\ 0, 1, 0, 0,\ 1\right\}^T,\ \boldsymbol{F_k} = EAL\boldsymbol{Q}^T \boldsymbol{B}_0^T. \tag{11}$$

where $\boldsymbol{M}$ is the cable element mass matrix, ρ and A are the material density and cross section area of the cable element, respectively. E is the Young's modulus of the cable element, $\boldsymbol{K}$ is the stiffness matrix of the element in the global coordinate system, β and γ are the Rayleigh damping coefficients, $\boldsymbol{F_g}$ is the equivalent nodal gravity force vector and g is the acceleration due to gravity.

The NP-FEM has an extra equivalent nodal elastic force vector $\boldsymbol{F_k}$ that does not exist in the usual FEM. It results from transforming the state variables from nodal displacement to nodal position and is the function of element rigidity EA and orientation only. The $\boldsymbol{K}$ and $\boldsymbol{F_k}$ quantities are highly nonlinear and time-dependent as the coordinate transformation matrix $\boldsymbol{Q}$ is function of the cable element orientation, which varies in time (Sun et al. [1]). The current approach calculates the strain energy directly by comparing the new element length to its undeformed one using the nodal position. Thus, it eliminates the source of accumulation error due to large rigid body rotation and, therefore, there is no geometric stiffness matrix in NP-FEM formulation (Sun et al. [1]).

Finally, the resulting system of equations is defined as (Zhu [3]):

$$\boldsymbol{M\ddot{X}_e} + \boldsymbol{C\dot{X}_e} + \boldsymbol{KX_e} = \boldsymbol{F_k} + \boldsymbol{F_g}. \tag{12}$$

Equation (12) is highly nonlinear due to the damping and stiffness matrices on the left-hand side, and the force vectors on the right-hand side are all functions of the current position $\boldsymbol{X_e}$.

3 Dynamics of towed body

The towed body is modeled as a rigid body with six degrees of freedom, defined by the position of its center of gravity (CG), described by (X_b, Y_b, Z_b) in the global coordinate system, and also by its orientation, using Euler angles (θ_x – roll, θ_y – pitch, θ_z – yaw) in a body fixed local coordinate system (x, y, z) with the origin at the body CG as shown in Fig. 2. The transformation order from the global to the local coordinate systems is defined as yaw, pitch and roll (Sun et al. [1]).

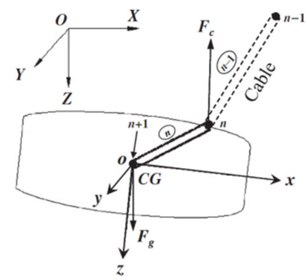

Figure 2. Schematic view of loads and coordinate systems of the towed body (based on Sun et al. [1])

Once the coordinate systems have been defined, the equation of translational motion of the towed body can be expressed in the global coordinate system while the equation of rotational motion can be expressed in the local coordinate system, respectively (Sun et al. [1]):

$$\boldsymbol{M_b}\ddot{\boldsymbol{X}}_{\boldsymbol{b}} = \boldsymbol{F_c} + \boldsymbol{F_g}, \tag{13}$$

$$\tilde{\boldsymbol{I}}\dot{\boldsymbol{\omega}} + \boldsymbol{\omega} \times \boldsymbol{H} = \boldsymbol{\tau_c} + \boldsymbol{\tau_b}, \tag{14}$$

with:

$$\boldsymbol{M_b} = \begin{bmatrix} m & 0 & 0 \\ 0 & m & 0 \\ 0 & 0 & m \end{bmatrix}, \tilde{\boldsymbol{I}} = \begin{bmatrix} I_{xx} & -I_{xy} & -I_{xz} \\ -I_{xy} & I_{yy} & -I_{yz} \\ -I_{xz} & -I_{yz} & I_{zz} \end{bmatrix}, \boldsymbol{H} = \begin{bmatrix} I_{xx} & -I_{xy} & -I_{xz} \\ -I_{xy} & I_{yy} & -I_{yz} \\ -I_{xz} & -I_{yz} & I_{zz} \end{bmatrix} \begin{Bmatrix} \omega_x \\ \omega_y \\ \omega_z \end{Bmatrix}. \tag{15}$$

where m is the mass of the towed body, (I_{xx}, I_{yy}, I_{zz}, I_{xy}, I_{yz}, I_{zx}) are the components of the moment of inertia tensor evaluated at its CG in the local coordinate system, $\boldsymbol{\omega} = \left(\omega_x, \omega_y, \omega_z\right)^T$ is the angular velocity vector of the towed body in the local coordinate system, ($\boldsymbol{F_c}$, $\boldsymbol{F_g}$) are the cable tension and gravity force acting on the towed body, ($\boldsymbol{\tau_c}$,) is the induced moment by the cable tension, and the dot above the variables denotes time derivative (Sun et al. [1]).

As showed by Sun et al. [1], one can have:

$$\dot{\boldsymbol{\omega}} = \boldsymbol{A}\ddot{\boldsymbol{\theta}} + \boldsymbol{B}, \tag{16}$$

$$\ddot{\boldsymbol{\theta}} = \begin{Bmatrix} \ddot{\theta}_x \\ \ddot{\theta}_y \\ \ddot{\theta}_z \end{Bmatrix}, \boldsymbol{A} = \begin{bmatrix} 1 & 0 & -\sin\theta_y \\ 0 & \cos\theta_x & \sin\theta_x\cos\theta_y \\ 0 & -\sin\theta_x & \cos\theta_x\cos\theta_y \end{bmatrix}, \boldsymbol{B} = \begin{Bmatrix} -\dot{\theta}_y\dot{\theta}_z\cos\theta_y \\ -\dot{\theta}_x\dot{\theta}_y\sin\theta_x + \dot{\theta}_x\dot{\theta}_z\cos\theta_x\cos\theta_y - \dot{\theta}_z\dot{\theta}_y\sin\theta_x\cos\theta_y \\ -\dot{\theta}_y\dot{\theta}_x\cos\theta_x - \dot{\theta}_z\dot{\theta}_x\sin\theta_x\cos\theta_y - \dot{\theta}_z\dot{\theta}_y\cos\theta_x\sin\theta_y \end{Bmatrix}. \tag{17}$$

Substituting Eq. (16) into Eq. (14) and multiplying both sides of the resulting expression by $\boldsymbol{A}^T$, the equation of rotational motion of the towed body is obtained in terms of Euler angles (Sun et al. [1]):

$$\left(\boldsymbol{A}^T\tilde{\boldsymbol{I}}\boldsymbol{A}\right)\ddot{\boldsymbol{\theta}} = \boldsymbol{A}^T\left(\boldsymbol{\tau_c} + \boldsymbol{\tau_b} - \boldsymbol{\omega} \times \boldsymbol{H} - \tilde{\boldsymbol{I}}\boldsymbol{B}\right). \tag{18}$$

The rigid body is connected to the cable physically by a spherical joint located at the top of the towed body. To couple the equation of motion of the cable Eq. (12) with the equation of motion of the towed body (Eqs. (13) and (18)), a massless rigid cable element is used to link the towed body CG to the end of the cable, as shown in Figure 2. The rigid cable element is a special case of the cable element with the rigidity of the element EA becoming infinite (Sun et al. [1]). In the simulation, a very large value of rigidity with respect to the elastic cable element is used. The system of equations is then (Sun et al. [1]):

$$\begin{bmatrix} \boldsymbol{M_c} & \boldsymbol{0} & \boldsymbol{0} \\ \boldsymbol{0} & \boldsymbol{M_b} & \boldsymbol{0} \\ \boldsymbol{0} & \boldsymbol{0} & \boldsymbol{A}^T\tilde{\boldsymbol{I}}\boldsymbol{A} \end{bmatrix} \begin{Bmatrix} \ddot{\boldsymbol{X}}_{\boldsymbol{C}} \\ \ddot{\boldsymbol{X}}_{\boldsymbol{b}} \\ \ddot{\boldsymbol{\theta}} \end{Bmatrix} + \begin{bmatrix} \beta\boldsymbol{M_c} + \gamma\left(\boldsymbol{K_c} + \tilde{\boldsymbol{K}}_{\boldsymbol{r}}\right) & \boldsymbol{0} & \boldsymbol{0} \\ \boldsymbol{0} & \beta\boldsymbol{M_b} + \gamma\boldsymbol{K_r} & \boldsymbol{0} \\ \boldsymbol{0} & \boldsymbol{0} & \beta\boldsymbol{A}^T\tilde{\boldsymbol{I}}\boldsymbol{A} \end{bmatrix}$$
$$\times \begin{Bmatrix} \dot{\boldsymbol{X}}_{\boldsymbol{C}} \\ \dot{\boldsymbol{X}}_{\boldsymbol{b}} \\ \dot{\boldsymbol{\theta}} \end{Bmatrix} + \begin{bmatrix} \boldsymbol{K_c} + \boldsymbol{K_{rr}} & \boldsymbol{K_{cr}} & \boldsymbol{0} \\ \boldsymbol{K_{cr}^T} & \boldsymbol{K_{r2}} & \boldsymbol{0} \\ \boldsymbol{0} & \boldsymbol{0} & \boldsymbol{0} \end{bmatrix} \begin{Bmatrix} \boldsymbol{X_C} \\ \boldsymbol{X_b} \\ \boldsymbol{\theta} \end{Bmatrix} = \begin{Bmatrix} \boldsymbol{F_c} \\ \boldsymbol{F_b} \\ \boldsymbol{\tau_b} \end{Bmatrix}, \tag{19}$$

where $\boldsymbol{X_c}$ is a $3n$-dimension vector containing all the nodal coordinates of cable, n is total number of nodes along the cable, $\boldsymbol{X_b}$ and $\boldsymbol{\theta}$ are 3-dimension vectors containing the towed body CG position and rotation angles, respectively. $\boldsymbol{F_c}$ is the total external load vector acting on the cable, while $\boldsymbol{F_b}$ and $\boldsymbol{\tau_b}$ are the external load and moment vectors defined in the right hand side of Eqs. (13) and (18). $\boldsymbol{M_c}$ is the assembled global mass matrix of cable and $\boldsymbol{M_b}$ is the mass matrix of towed body defined in Eq. (13). Similarly, $\boldsymbol{K_c}$, is the assembled global stiffness matrix of the cable. The stiffness sub-matrices associated with the rigid cable element, $\boldsymbol{K_{r1}}$, $\boldsymbol{K_{r2}}$ and $\boldsymbol{K_{cr}}$, are constructed as (Sun et al. [1]):

$$K_{6\times 6}^{rigid} = Q^T K_0 Q = \begin{bmatrix} K_{r1(3\times 3)} & K_{r0(3\times 3)} \\ K_{r0(3\times 3)}^T & K_{r2(3\times 3)} \end{bmatrix}_{6\times 6}, K_{rr} = \begin{bmatrix} \mathbf{0}_{3(n-1)\times 3(n-1)} & \mathbf{0}_{3(n-1)\times 3} \\ \mathbf{0}_{(3\times 3)(n-1)} & K_{r1(3\times 3)} \end{bmatrix}_{3n\times 3n}, K_{cr} = \begin{bmatrix} \mathbf{0}_{3(n-1)\times 3} \\ K_{r0(3\times 3)} \end{bmatrix}_{3n\times 3}. \quad (20)$$

The boundary conditions for Eqs. (12), (13) and (18) are the motion of the tow point, which are provided as prescribed positions (X, Y, Z) varying with time. The system of equations of motions is solved over time using the alpha-generalized method (see Kuhl and Crisfield [5]) in order to maintain numerical stability for nonlinear applications.

4 Applications

4.1 Free fall of flexible cable

This example considers a flexible cable suspended between two pinned ends, being suddenly released from one end and swinging freely about the other end (Ding et al. [2]). The physical properties are described as follows: section area A = 1.962 x 10^{-5} m², length l = 1.713 m, density ρ = 7800 kg/m³, effective Young's modulus E = 53 GPa, mass m = 0.34 kg, and gravitational acceleration g = 9.81 m/s².
In the same manner as Ding et al. [2], the cable was modeled using 24 elements with a time step of 2x10^{-6} s. The spectral radius is fixed to 0.3. The boundary and initial conditions for this problem are as follows: $X = Y = Z = 0$ at the pinned joint, $V_X = V_Y = V_Z = 0$ and $a_X = a_Y = a_Z = 0$. Damping is not considered here. Results are shown in Fig. 3, where the position of the free end is presented over time. As it can be seen, the results agree very well with predictions obtained by Ding et al. [2], and with the commercial software LS-DYNA. Figure 4 shows some snap shots of the cable from t = 0 s up to 2.8 s, showing a lot of resemblance with the reference results.

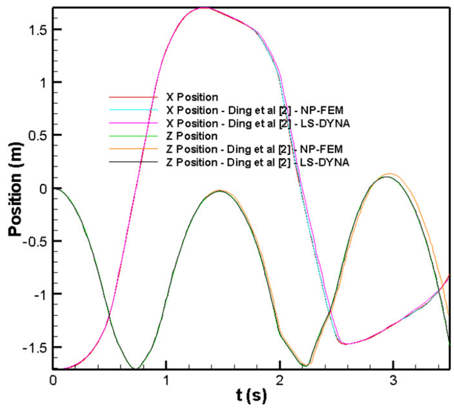

Figure 3. Horizontal (X) and vertical (Z) positions of the end point of the free fall undamped cable

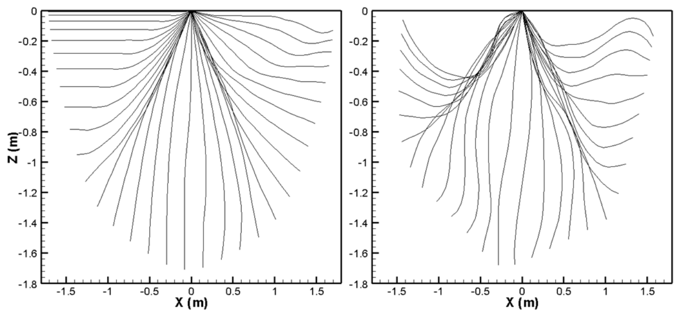

Figure 4. Shapes of undamped cable free fall

4.2 Flexible polyethylene rubber conical pendulum

The next example shows a pendulum describing a circular motion, as showed by Fig. 5. It has a lumped mass m of 0.3 kg attached to the end of the rod. The pendulum density is ρ = 1300 kg/m³, Young's modulus E = 7.8 MPa, cross-sectional area A = 1 x 10^{-5} m², length L = 2,0 m and the acceleration of gravity g = 9.8 m/s². The vertical direction of the pendulum is defined by $\theta = \pi/3$ rad, the rotational radius is $r = \sqrt{3}/2$m, the pendulum is initially set to the $X = 0$ plane. The initial tangential velocity of the mass is $V_0 = 5.42218$ m/s along the positive direction of the X-axis. The pendulum rod is modeled by 10 elements with the same length. The time step is $\Delta t = 2 \times 10^{-4}$ s, the spectral radius is 0.7 and the simulation interval is 10 s.

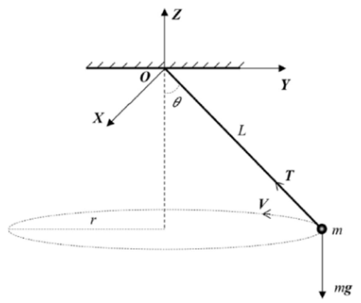

Figure 5. The flexible conical pendulum (Ding et al. [4])

Figure 6 presents the time histories of displacement and velocity of the lumped mass. As it can be seen, it agrees very well with the results shown by Ding et al. [4].

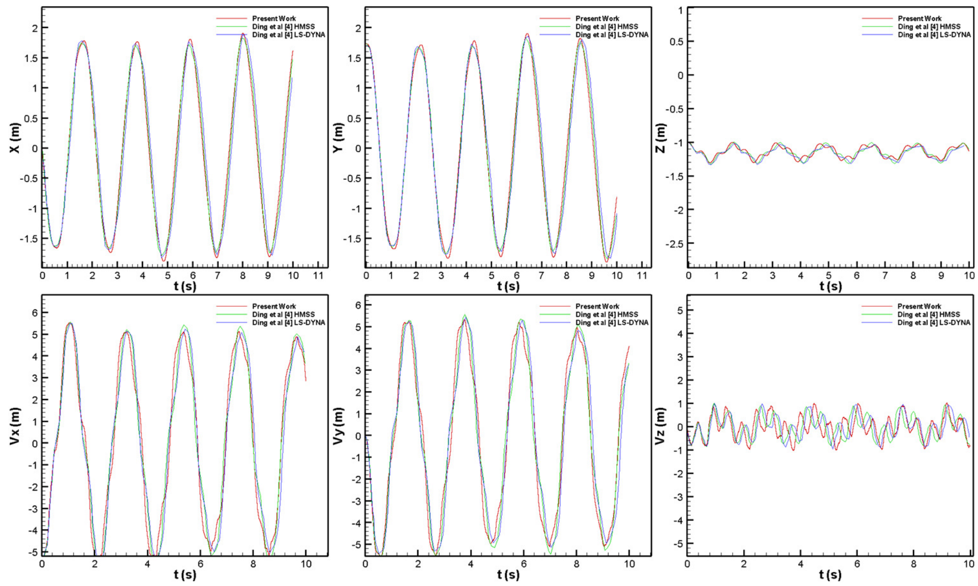

Figure 6. Displacement and velocities of the lumped mass

4.3 Cable-Rigid body pendulum

The final example tests the cable formulation when it is attached to a rigid body. The pendulum shown in Fig. 7 consist of a rod with length $l = 1.713$ m and specific mass $\rho = 3.215$ kg/m³, cross section $A = 1.962\text{x}10^{-4}$ m² and Young's modulus $E = 5.3\text{x}10^{10}$ Pa. The attached rigid body have mass $m = 0.01$ kg, rotational inertia $I = 1.698$ $\text{x}10^{-5}$kg.m² and is released with an initial angular acceleration $\alpha_0 = -3.884$ $\text{x}10^{-1}$ rad/s^2. The pendulum is released at the initial angle $\theta_0 = 86°$. The acceleration gravity is $g = 9.81$ m/s². The time step is $2\text{x}10^{-6}$ s and the spectral radius is 0.8. The rigid body has cubic shape with initial CG position at X = -0.123 m, Y = -1.759 m and Z = 0m.

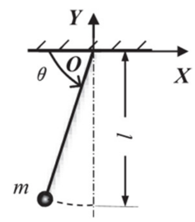

Figure 7. Cable-Rigid body pendulum (based on Ding et al. [4])

Numerical results were verified through comparison with the classical analytical solution of a simple pendulum.

Although there are differences between the two models (i.e. the classical pendulum does not include deformation of the rod and the body is treated as a simple lumped mass), the results were quite similar, as shown in Fig. 8 for the rigid body, making possible the comparison.

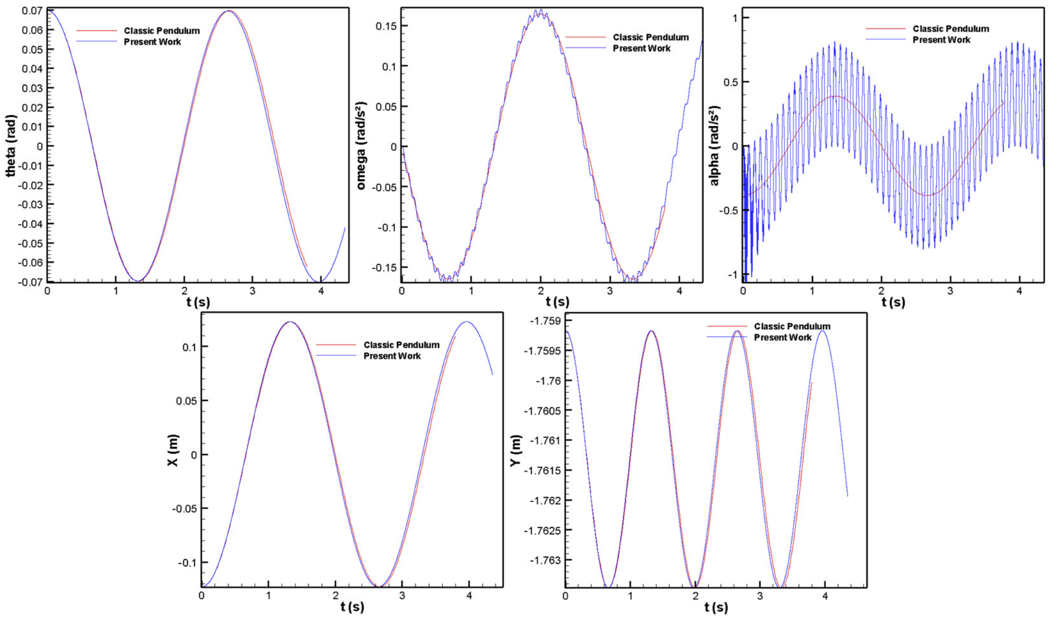

Figure 8. Comparisons of angular rotation, velocity and acceleration, and horizontal (X) and vertical (Y) positions for the cable-rigid body pendulum

5 Conclusions

A numerical formulation based on NP-FEM has been developed to solve non-linear problems involving cable-rigid-body structural systems. The method eliminates accumulated errors over time observed in displacements formulations. Also, the cable is coupled with the body through the use of a rigid link between the cable free end and the CG of the rigid body. Simulations results show that the implemented method is capable of simulating towed-cables with high accuracy, proving efficacy, reliability and stability of the present formulation.

Acknowledgements. The authors would like to thank CNPq and CAPES for their financial support to this ongoing research, as well as to CESUP and CENAPAD-SP for assistance, technical support and computational resources provided.

Authorship statement. The authors hereby confirm that they are the sole liable persons responsible for the authorship of this work, and that all material that has been herein included as part of the present paper is either the property (and authorship) of the authors, or has the permission of the owners to be included here.

References

[1] F. J. Sun, Z. H. Zhu and M. LaRosa. “Dynamic modeling of cable towed body using nodal position finite element method”. Ocean Engineering, vol. 38, pp. 529-540, 2011.
[2] H. Ding, Z. H. Zhu, X. Yin, L. Zhang, G. Li and W. Hu. “Hamiltonian Nodal Position Finite Element Method for Cable Dynamics”. International Journal of Applied Mechanics, vol. 9, n. 8, pp. 1-20, 2017.
[3] Z. H. Zhu. “Dynamic modeling of cable system using nodal position finite element method”. International Journal for Numerical Methods in Biomedical Engineering, vol. 26, pp. 692-704, 2010.
[4] H. Ding, X. Yin, Z. H. Zhu and L. Zhang. “A high accurate hamiltonian nodal position finite element method for spatial cable structures undergoing long-term large overall motion”. Communications in Nonlinear Science and Numerical Simulation, vol. 70, pp. 203-222, 2019.
[5] D. Kuhl and M. A. Crisfield. “Energy-conserving and decaying algorithms in non-linear structural dynamics”. International Journal for Numerical Methods in Engineering, vol. 45, pp. 569-599, 1999.